

ATOMIC STRUCTURE AND NONELECTRONIC PROPERTIES OF SEMICONDUCTORS

Genesis of Nanoscale Defects and Damage in GaAs Subjected to Multipulse Quasi-Static Photostrains in Micrometer-Sized Regions of Semiconductor

S. V. Vintsents*, A. V. Zaitseva**, V. B. Zaitsev**, and G. S. Plotnikov**

**Institute of Radio Engineering and Electronics, Russian Academy of Sciences (Fryazino Branch), pl. Vvedenskogo 1, Fryazino, Moscow oblast, 141120 Russia*

e-mail: vintsents@mail.ru

***Moscow State University (Faculty of Physics), Vorob'evy gory, Moscow, 119899 Russia*

Submitted May 13, 2003; accepted for publication May 19, 2003

Abstract—Atomic-force microscopy and analysis of both photothermal (quasi-static) strains of surfaces and the kinetics of intensity of specularly reflected light were used to study special features of defect production in GaAs in relation to the number N of focused laser pulses incident on the surface. Irradiation of the semiconductor was accompanied by its electronic excitation, local heating, and deformation of surface layers. It is shown for the first time that the genesis of surface defects and damage in semiconductors (within the laser spot with a micrometer diameter) has a multistage character in the vicinity of the plasticity threshold. The defect-induced and plastic nanometer-scale surface displacements ΔU_z increase with increasing N only if the shearing surface strains ϕ exceed the previously determined values $10^{-5} < \phi_0 < 10^{-4}$ for deformation-related elasticity (quasi-elasticity) limits in GaAs. The origination of nanoscale defects and their self-organization at the early stages of photostrains in the semiconductor is discussed. The possible relation between the defects observed and the subsequent catastrophic damage to micrometer-sized regions of GaAs at large values of N is considered.
© 2004 MAIK "Nauka/Interperiodica".

1. INTRODUCTION

The interaction of pulsed laser radiation with a GaAs surface has been studied for more than 20 years. The persistent interest in this interaction is caused by the wide use of gallium arsenide in modern microelectronics and optoelectronics [1] and also, in particular, by the fact that nonequilibrium pulsed laser irradiation can initiate various phase transformations in semiconductors and affect a number of properties of the surface layer within the irradiated zone [2, 3]. When interacting with GaAs, optical radiation irreversibly changes the chemical composition and microstructure of this compound [2–6], as well as its luminescent [3, 7, 8] and electrical [6, 7, 9] characteristics, and it stimulates the generation of point and extended defects [7, 10, 11] and affects the properties of oxide layers [2, 3, 12] and the surface profile [13, 14].

The single-shot irradiation of semiconductors with nanosecond laser pulses (or laser pulses with other widths) in the spectral region of the band-to-band absorption of light was used in the majority of early studies; the density W of the incident energy was varied. The irradiated areas were comparatively large (typically, larger than 1–10 mm²); the distribution of optical-radiation intensity was quasi-uniform throughout the irradiated area, which ensured that there were no shearing strains within this area. Variations in the semi-

conductor properties were caused mainly by the generation of defects and were observed near the surface; for these variations to occur, the incident-energy density W in the pulses should have been close to the calculated thresholds W_m for the formation of the surface (metastable) liquid phase [2, 3]. The results were predominantly explained by the thermal effect of illumination [2–6] or the combined effect that involved (for $W < W_m$) electronic excitations in the semiconductor [7, 10].

In order to gain insight into the contribution of photostrains to the production of defects, we carried out direct photostrain studies of semiconductors and metals using a different approach. This is based on the use of localized and multiple moderate-energy focused single-mode irradiation events with controlled and almost Gaussian light-intensity distribution [15–18]; i.e., we have $I(r, t) = W \exp(-r^2/\omega^2)(t/\tau^2) \exp(-t/\tau_0)$, where $W = 10\text{--}100 \text{ mJ/cm}^2 \ll W_m$ is the incident-energy density at the laser-spot center, $\omega = 10\text{--}100 \text{ }\mu\text{m}$ is the laser-spot radius at the sample surface, and $\tau = 0.1\text{--}1 \text{ }\mu\text{s}$ is the characteristic width of the pulses. As expected, we observed an appreciable increase in the strain-related effects. Specifically, we observed the low-threshold effect of shearing strains and stresses that arise due to local irradiation on point-defect production in the surface layers of germanium and silicon [19–22].

Naturally, controlled photodeformation effects in the vicinity of previously detected deformation-related

limits of elasticity (quasi-elasticity) in semiconductors $\phi_0(W_0)$ [21–25] attract particular interest. Our previous publications concerned with the aforementioned effects included primarily electrical and optical studies of Ge and Si under conditions of laser scanning of actual surfaces. The number of laser pulses was maintained constant ($N \approx 10^3$), whereas the value of W was varied [19–22]. At the same time, the number N of laser pulses can be considered as one of the most natural control parameters (along with the energy density W). Therefore the study of the earliest stages of defect production (when N is still small) is of most interest. In order to simplify the interpretation of the results, it is appropriate to carry out the measurements in the absence of laser scanning, i.e., when the laser-beam position at the surface is fixed.

Previously, we used X-ray and chemical microanalysis, electron microscopy, and Auger spectroscopy to study the situation where the laser-beam position at the GaAs surface was fixed and the value of N was large ($N \approx 10^5$ – 10^6) [26]. We found that GaAs was a more complex object than Ge or Si, mainly due to the volatility of arsenic [2, 3] and possible development of various low-threshold phenomena [26, 27]. Note, for example, that nonsteady (acoustic) strains initiated by localized irradiation induced decomposition of GaAs in a thin (~ 4 – 7 nm) surface layer. This decomposition gave rise to a nearly equal number of unbonded Ga and As atoms even at fairly large distances (on the order of millimeters) from the irradiated zone with a radius of $\omega \approx 20$ μm [26]. The long-range effect of laser pulses observed by Barskov *et al.* [26] was not related (as in [28]) to a nonsteady thermal field localized in the vicinity of the irradiated region. Indeed, some processes that vary quite slowly with time and are mainly related to the temperature gradients are dominant on the microsecond time scale within the laser-spot area; these processes are quasi-static and are referred to as photothermal strains of solid-state surfaces [16–25]. These slow shearing strains in pulsed photoacoustic spectroscopy of the laser-beam deflection [15–18] are typically characterized by the values of local inclinations of the strained surface $\phi \equiv (dU_z/dr)$, where U_z is the effective normal displacement of the surface and r is the distance from the beam center. When $\phi > \phi_0 \approx (5$ – $6) \times 10^{-5}$ and, accordingly, energy densities $W > W_0 \approx 100$ mJ/cm^2 [22], macrodamage (structural catastrophe) was previously observed in micrometer-scale GaAs regions [26]. Microcraters of regular circular shape with a depth of $\sim (1$ – $5)$ μm and radius $\omega = \sim 20$ μm were formed (mainly due to noncongruent evaporation of arsenic) at the GaAs surfaces within the laser spot at large values of N [26]. We emphasize that the genesis of earlier (initial) stages of defect production in local GaAs regions as the value of N increased has not yet been studied.

In this study, we used atomic-force microscopy (AFM) and analysis of both photothermal surface strains (PTSSs) and the intensity of specularly reflected light to gain insight for the first time into the process of

formation of finer, nanoscale variations in the GaAs surface profile as a result of multiple quasi-static photostrains in micrometer-sized regions of semiconductors in the vicinity of thresholds $\phi_0(W_0)$ [22] with wide ranges of variations in N (from unity to 10^5).

This study may be useful to justify the boundaries of nondestructive modes in GaAs laser microscopy [29] and to simulate the degradation processes in small-sized (1 – 10 μm) semiconductor optoelectronic devices (for example, those designed for millimeter-region wavelengths) subjected to local overheating [30, 31] and, as a consequence, to strains [32].

2. EXPERIMENTAL

The samples were 5×5 mm^2 in area, had a (100) orientation of the surface, and were cut from a single epitaxial GaAs structure composed of a 2.4 - μm -thick film with electron concentration $n \approx 10^{16}$ cm^{-3} . The film was grown by liquid-phase epitaxy on a heavily doped substrate ($n^+ \approx 10^{18}$ cm^{-3}) with a thickness of ~ 250 μm . Details of the preliminary preparation of the surface for irradiation were described in [26].

The GaAs samples were irradiated with focused laser pulses (without scanning the beam) in atmospheric air at room temperature. The second harmonic of a pulsed Nd:YAG laser with wavelength $\lambda = 0.53$ μm and characteristic pulse width $\tau \geq 0.4$ – 0.5 μs was used for irradiation. The total pulse width at a 0.1 level of I_{max} was no smaller than 1.5 μs . The pulse-repetition rate was $f = 10$ – 25 kHz ; the pulse train could be interrupted using a shutter with the exposure time Δt_i ranging from 0.005 to 10 s. The single-mode laser radiation was focused on GaAs samples to a spot with a regular shape and Gaussian radius $\omega \approx 20$ μm . The spot size was monitored during irradiation using the PTSS method [16] to reveal characteristic profiles of arising quasi-elastic strains; an SOK-1-01 optical microscopy accessory was also used [23].

The incident-energy density $W = E/\pi\omega^2$ (E is the total energy in a pulse) ranged from 10 to 350 mJ/cm^2 at the laser-spot center; the range of variations in W was chosen so that the previously ascertained thresholds for the origination of inelastic strains in GaAs surface layers ($W_0 \approx 100$ mJ/cm^2 [22]) were within this range. We emphasize that, for the microsecond laser pulses used in this study, the calculated [3] melting thresholds for GaAs $W_m \geq 1$ – 1.2 J/cm^2 were much higher than those for pulses with well-studied nanosecond-scale values of τ ($W_m \approx 200$ mJ/cm^2) [2, 3].

In order to study the kinetics of large-scale damage within the laser spot (0.1 – 1 μm), we used the PTSS method [16, 23] and relied on the time dependence of integrated intensity $I_p(t)$ of the probe He–Ne laser beam reflected specularly from the semiconductor surface under a continuous train of focused laser pulses. We paid special attention (as in [33]) to steady-state values of $I_p(t)$ attained in the time intervals between the pulses.

The point in time t_0 at which the ratio $I_p(t_0)/I_p(0)$ decreased irreversibly to the level of 0.9 was considered as the onset of catastrophic damage. A new (undamaged) GaAs region was chosen each time for repeated recording of the $I_p(t)$ kinetics, which was monitored using an SOK-1-01 microscope. The method for determining t_0 and, accordingly, the critical number of irradiating laser pulses $N_0 = ft_0$ was also described previously [34, 35].

In order to study the earlier stages of defect production in GaAs (i.e., at $N \ll N_0$), we used an AFM system and an optical microscope, which were incorporated into the equipment supplied with a Nanoscope-111a (Digital Instruments) scanning probe microscope. Individual areas of the semiconductor (with a small number of pulses N) were subjected to local pulsed irradiation with fixed energy densities W_i , where $W_i/W_0 = 0.1, 0.9, 1.15, 1.35, 1.6, 2.0, 2.6, 3.0$, and 3.5 . In this case, the number of pulses N was varied by varying the irradiation time Δt_i (see above). An array of photoirradiated GaAs regions obtained on a single epitaxial structure made it possible to study special features of the defect-producing surface strains and the nanoscale damage that formed in relation to both W at $N = \text{const}$ and the number of laser pulses N at a fixed energy density W_i .

The resolution of the optical microscope made it possible to observe only the most radical variations in the surface profile at a level of irreversible displacements $\Delta U_z \approx 1 \mu\text{m}$. Atomic-force microscope was used to study a finer evolution of the surface nanopile ($\Delta U_z \approx 1 \text{ nm}$) at the early stages of deformation (small N and $W \approx W_0$). The AFM measurements were performed in atmospheric air. The microscope operated in the contact mode; the rigidity of levers was $0.01\text{--}0.2 \text{ N/m}$. The AFM images were processed and analyzed using a FemtoScan-0.01 special software package [36].

3. RESULTS AND DISCUSSION

3.1 Boundaries of Defect-Producing Inelastic Strains

As noted previously [22–25], the controlled inelastic processes initiated in semiconductors by multiple pulsed laser irradiation of micrometer-sized areas are limited from below in the energy density W by the region of reversible linear photoacoustics (thresholds W_0), and are limited from above by uncontrolled damage-forming processes (W_d thresholds). At $W_0 < W < W_d$ and $\omega = 10\text{--}100 \mu\text{m}$, the number N of laser pulses becomes an important parameter of inelastic effects [22].

In this context, we studied in GaAs primarily the dependences of the upper thresholds W_d on N using the methods described previously [34, 35] (Fig. 1). To this end, we measured the kinetics $I_p(t)$ at $W < W_0 = 90\text{--}100 \text{ mJ/cm}^2$ (case 1, Fig. 1a, curve 1) and at $W > W_0$ (case 2, Fig. 1a, curve 2). In case 1, we failed to detect appreciable variations in $I_p(t)$ for $N \geq 10^7\text{--}10^8$ in the intervals between the pulses. In case 2, we determined the critical number of pulses N_0^i (Fig. 1a, curve 3) and

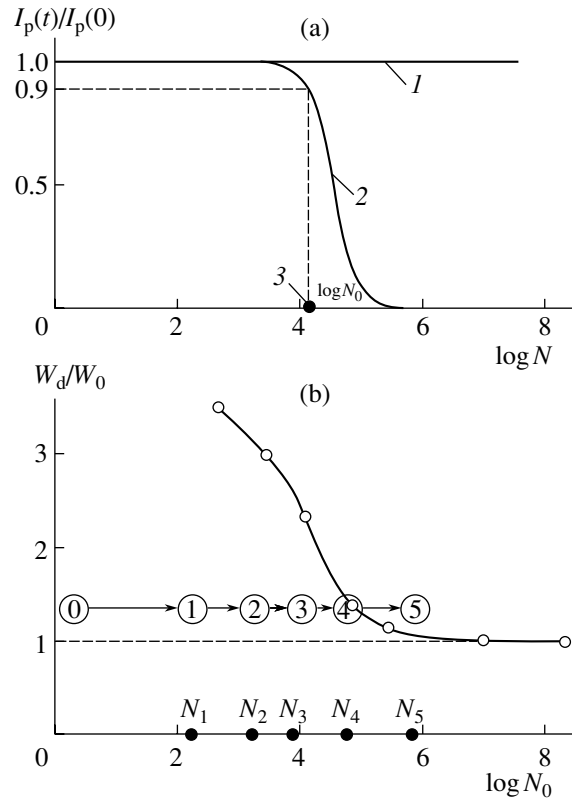


Fig. 1. (a) Kinetics $I_p(t)$ of the intensity for a continuous probing laser beam reflected specularly from the semiconductor (normalized to the initial intensity $I_p(0)$): (1) in the mode of nondestructive quasi-elastic photostrains in GaAs, $\varphi < \varphi_0$ ($W < W_0$); (2) with destructive irradiation of the semiconductor, $\varphi > \varphi_0$ ($W > W_0$); and (3) the scheme for determining the critical number of laser pulses N_0 . (b) Dependence of the damage thresholds W_d (in units of $W_0 = 90\text{--}100 \text{ mJ/cm}^2$) on $\log(N_0)$ for GaAs at $\omega \approx 20 \mu\text{m}$. The numbers 0–5 illustrate the trend for an increase in N at $W/W_0 \approx 1.35$. Numerical values of N_i are listed in the table.

then plotted the dependences of W_d^i on N_0^i for several (i) fixed destructive levels of the energy density $W_0 < W_d^i < 3.5W_0$ (Fig. 1b). We emphasize that appreciable degradation and catastrophic damage in micrometer-sized irradiated semiconductor regions always developed when N exceeded N_0 ; furthermore, we had $I_p(t) \rightarrow 0$ when $N \rightarrow \infty$ (Fig. 1a).

It can be seen from the experimental dependence $W_d(N)$ shown in Fig. 1b that there is a sharp boundary that is located at $W \approx W_0$ and separates the irradiation-induced regions of degradation of the semiconductor from relatively nondestructive irradiation levels. In order to make certain that precisely the mode of quasi-elastic strains in GaAs was realized under the conditions of our experiments at $W < W_0 = 90\text{--}100 \text{ mJ/cm}^2$, we used (as in [22, 26]) the PTSS method (Fig. 2a). Using this method, we managed to confirm the view that, at $\varphi \equiv (dU_z/dr)_{\text{max}} < \varphi_0 \approx 5\text{--}6 \times 10^{-5}$, the photo-

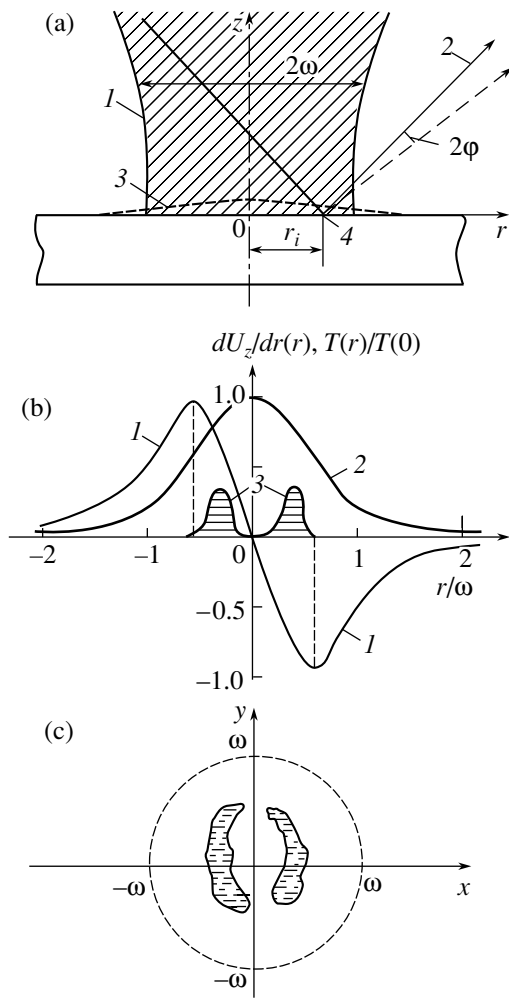


Fig. 2. (a) Schematic representation of the PTSS method [16, 22]: (1) a pulsed single-mode “heating” laser beam with a diameter of $\sim 2\omega$, (2) a continuous probing laser beam whose deflection $2\phi(r, t)$ from the strained surface 3 is measured at various points (4) of the surface r_i . (b) Typical distributions of (1) quasi-static shearing strains $\phi(r) \equiv dU_z/dr(r)$ arising in GaAs at $W \leq W_0$ [26] and (2) normalized calculated temperature $T(r)/T(0)$ over the cross section of the “heating” beam; (3) radial distribution of primary damaged regions detected at $W \geq W_0$. (c) Schematic representation of damaged regions within the irradiated zone of GaAs; this scheme was derived on the basis of the combined data obtained using the AFM method.

strains $\phi(t)$ in GaAs are indeed completely reversible in time, and the features of the photostrain’s kinetics do not vary from pulse to pulse up to $N \geq 10^7$ – 10^8 [22].

Since the shearing strains dU_z/dr may play a significant role in the mechanisms of point defect production and catastrophic damage in monatomic semiconductors and metals [19–25], we used the PTSS method [16] to study the features of the $\phi(r)$ distribution over the beam cross section for GaAs (Fig. 2b, curve 1). The largest strains were observed at the time instants that corresponded to the completion of laser pulses $t = 1.5$ – 2.0 μ s, i.e., to the time instants that corresponded to the com-

pletion of the main heat release in the semiconductor [2, 3]. The maximal values of ϕ were shifted in reference to the beam cross-section center by $r_{\max} \approx \omega/\sqrt{2} = 12$ – 15 μ m. Note that the similar distribution $\phi(r)$ in metals at early stages of strain development was previously related to a partial accomplishment of “quasi-single-mode” conditions of displacements $U_z(r)$ [17, 18].

Thus, the preliminary study of the kinetics $I_p(t, W)$ and strains $\phi(t, r, W)$ made it possible to correctly choose the modes of studying the early stages of defect production and nanodamage in GaAs in coordinates (W, N) . Defect production under the aforementioned conditions ($W/W_0 \geq 1$ and $N/N_0 \ll 1$) for various values of N was thereafter studied using the AFM method.

The genesis of nanometer-sized defects and damage in GaAs was studied for various combinations of the values of W and N . As an example, we used the numbers from 0 to 5 to illustrate the trajectory of the increase in N for $W/W_0 \approx 1.35$. The corresponding AFM results are shown in Figs. 3a–3d and are listed in the table. We managed to separate several different stages in the development of defect and damage production. Below, we describe the main characteristics of these stages in order of increasing N (numerical values of N_i for $W/W_0 \approx 1.35$ are listed in the table).

3.2. Time Interval Corresponding to the Latent Buildup of Defects

It is found that, with the smallest number of laser pulses ($N < N_1$), the latent buildup of point defects is dominant and the nanometer-scale amplitudes ΔU_z^0 of the random surface profile are retained; this profile is characteristic of unirradiated GaAs with $\Delta U_z^0 < 1$ nm. The method of dynamic indentation has been previously applied to certain semiconductors (among them, GaAs) to show [37] that, at short durations (≤ 1 – 10 ms) of pulsed contact loading, the dislocation-unrelated mechanisms of microplasticity in the surface layers with preferential point migration (rather than extended) defects near the surface are dominant. The defect-diffusion mechanisms of microplasticity are characteristic of relatively small near-surface stresses in semiconductors [19–22] and can be in effect at comparatively low temperatures (including 295 K) [38].

3.3. Stage 1

At $N_1 < N < N_2$, clusters of point defects are formed in the semiconductor regions shifted by $r = 6$ – 7 μ m to the periphery in reference to the irradiation-spot center (Fig. 2b, curves 3). These clusters are not oriented spatially and are related by the AFM method to a preferential reduction in the initial surface-profile amplitude in the semiconductor (Fig. 3a). The complex profile features are observed with a certain increase at the nanocrater center within each nanocrater. The difference in

heights ΔU_z for these defects amounts to 1.5–2.0 nm, and the characteristic dimension of surface-profile features is 10–50 nm (see table). The results of comparing the aforementioned characteristics of the defects with the previous data obtained using X-ray microanalysis [26] suggest that the detected local nanometer-scale depressions in the GaAs surface profile are mainly caused by an escape of arsenic from the semiconductor. Further development of early damage-formation stages and origination of new types of defects occurred mainly within the aforementioned peripheral regions (i.e., near the boundaries of the laser spot) (Fig. 1c) and was accompanied by the extension of these regions as N increased.

3.4. Stage 2

Spatial self-organization of unoriented clusters composed of nanometer-sized defects along one of the crystallographic axes in GaAs was observed at $N_2 < N < N_3$ (Fig. 3b). Depression regions (with $\Delta U_z = 5$ –7 nm) in the profile merge into fairly thin (50–100 nm) and extended (400–600 nm) lines with a spatial period of 100–200 nm (Fig. 3b, table). We emphasize that the above processes continue to be predominant at distances $r_0 = 5$ –10 nm from the laser-spot center (Fig. 2b, curve 3, Fig. 2c) rather than at the center itself, where a photoinduced increase in the temperature $\Delta T(r)$ and the concentration of nonequilibrium electrons are maximal [2, 3, 15–18, 23] (Fig. 2b, curve 2). These observations clearly indicate that not only the temperature $\Delta T(r)$ and electronic excitation of semiconductors but also local shearing quasi-static strains $\phi \equiv dU_z/dr$ contribute significantly to the processes of defect production and redistribution under investigation (Fig. 2b, curve 1). Indeed, the regions of origination (stage 1) and primary self-organization (stage 2) of the defects under conditions of local photodeformation of GaAs were always found between the peaks of $\Delta T(r)$ and $\phi(r)$ (Fig. 2b, curves 1–3). Such a multifactorial character of point defect formation was previously studied in detail for quasi-single-mode conditions of irradiation of semiconductor with nanosecond laser pulses; an electronic–deformational–thermal model was suggested to interpret the experimental data [39–41]. The effects of self-organization of defects are much less pronounced in radial directions (the y axis in Fig. 2c), which are perpendicular to the observed extended lines of defect clusters (Fig. 3b). This fact suggests that the defect clusters migrate (and then merge together) more easily along a certain crystallographic direction, which was detected using the AFM method; the above orientational behavior can be attributed, e.g., to the piezoelectric effect [1–3]. The aforementioned directions can correspond to projections of piezoelectric axes onto the (100) plane. Apparently, the shearing strains dU_z/dr and subsurface stresses σ_{xz} [23–25] that are perpendicular to these directions (Fig. 2c) may be much less efficient.

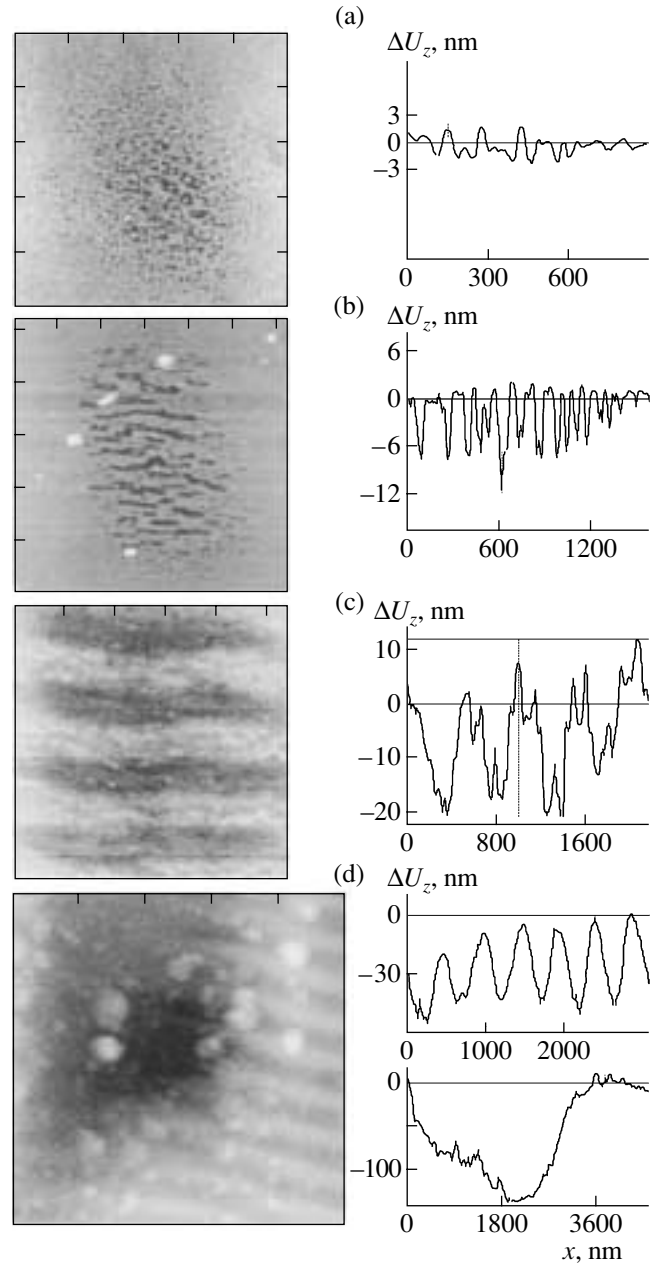


Fig. 3. AFM images of GaAs surface areas at various stages of defect formation under conditions of multiple quasi-static deformation of the semiconductor. The size of the imaged area is (a–c) $2 \times 2 \mu\text{m}^2$ and (d) $4.5 \times 4.5 \mu\text{m}^2$. The profiles of the normal surface displacements $\Delta U_z(x)$ along the vertical direction z are shown on the right (x is the coordinate in the surface plane).

3.5. Stage 3

Enlargement of oriented bands in the GaAs surface profile occurs when $N_3 < N < N_4$ (Fig. 3c). A one-dimensional (1D) wavelike profile with a height difference $\Delta U_z = 15$ –20 nm a transverse (lateral) dimension of 200–250 nm, and a period of 400–500 nm is formed on a larger scale without changing the spatial orienta-

Consecutive stages of genesis of nanometer-sized defects in GaAs with increasing number N of destructive ($W/W_0 \approx 1.35$) quasi-static photostrains in the micrometer-sized regions of GaAs

Stage no.	The number N of pulsed quasi-static photostrains	The dominant type of generated defects	Characteristic sizes		
			the height difference ΔU_z , nm	lateral dimension, nm	the structure period, nm
0 (latent)	$1 < N < N_1$	Latent buildup of point defects at amplitudes of the displacement fluctuations $\Delta U_z < 1$ nm	$\Delta U_z^0 < 1$	-	-
1	$N_1 < N < N_2$	Unoriented clusters of nanodepressions at the surface	1.5–2	10–50	-
2	$N_2 < N < N_3$	Merging of the clusters into oriented bands of depressions	5–7	50–100	100–200
3	$N_3 < N < N_4$	Enlarged oriented waves of the surface nanoprofile	15–20	20–250	400–500
4	$N_4 < N < N_5$	Deepened waves of depressions in the surface nanoprofile	30–40	~250	~500
5	$N > N_5$	Local pitting (erosion) of GaAs, individual microcraters	100–150	≤ 1000	-
		A unified macroscopic crater (a catastrophe)	1–5	$(1-3) \times 10^4$	-

Note: The values of N were equal to $N_1 \approx (2-5) \times 10^2$, $N_2 \approx 2.5 \times 10^3$, $N_3 \approx 10^4$, $N_4 \approx (5-10) \times 10^4$, and $N_5 \geq 10^5-10^6$ under conditions of local pulsed laser irradiation of GaAs at $\omega \approx 20 \mu\text{m}$ and $W/W_0 \approx 1.35$ (see text).

tion of the bands (see table). In our opinion, although the period of the wavelike structures in stage 3 almost coincides with the wavelength λ , this period is not related to the phenomena of optical interference [2, 3, 29], since the period of similar structures observed in stage 2 was much shorter than λ (see text above and table). A predominant lowering of the surface profile (formation of depressions) occurs in stage 3 (as in previous stages); this lowering is apparently related to the continuing escape of arsenic from the semiconductor. Two established facts count in favor of this hypothesis. First, damage to the GaAs surface with a diameter of 10–15 μm is accompanied by the formation of sharp edges of the profile, with the height of these edges equal to 15–20 nm. It will be recalled that a similar effect was previously attributed to noncongruent evaporation of arsenic, which was corroborated by the observation of blue cathodoluminescence using an optical microscope in the microanalyzer in the region of the forming profile edge due to the origination of Ga_2O_3 in this region as a result of oxidation of unbonded gallium. Second, according to the AFM data, the remaining portion of unbonded gallium is involved in the formation of nanometer-sized drops in stage 3 in the direction of the y axis (Fig. 2c), which was predicted previously on the basis of stoichiometric data obtained by Auger spectroscopy of GaAs [26].

3.6. Stage 4

As the number N of the laser pulses incident on GaAs increased ($N_4 < N < N_5$), individual defects in the form of craters appeared at several sites of the semiconductor surface, mainly at distances $r \approx r_0$ from the laser-

spot center. One such defect has a fairly regular (circular) shape with a bottom depth of $\Delta U_z = 120-150$ nm and a transverse dimension of $\sim 1 \mu\text{m}$ and is shown in Fig. 3d. It was ascertained by the AFM method that such local pitting (erosion) of GaAs occurs only against a background of oriented enlarged profile bands with height difference $\Delta U_z \geq 30-40$ nm (Fig. 3d). These bands were already formed at stage 3 and are additionally developed in stage 4. Comparison of the AFM data on $N = N_4$ and the dependences $W_d(N)$ at $W/W_0 \approx 1.35$ in Fig. 1 suggests that it is the observed stage 4 that should be identified with the onset of catastrophic degradation of GaAs. It should be recalled that the thresholds W_d of the aforementioned damage were conventionally determined previously in semiconductors and metals either from irreversible decrease in the intensity of specularly reflected light or using various versions of optical microscopy [23–25, 29, 34, 35]. In this study, we used the AFM method on the nanometer scale of surface displacements to monitor for the first time the earlier stages (stages 1–3) of defect production in micrometer-sized regions of GaAs.

3.7. Stage 5

Individual microcraters that had arisen at stage 4 merged into a single macroscopic defect at $N > N_5 = 10^5-10^6$. As a result, a “giant” circular crater was formed. This crater had a depth of $\Delta U_z = 1-5 \mu\text{m}$ and a transverse dimension of 10–30 μm ; the latter was close to the diameter 2ω of the laser spot at the semiconductor surface. Previously, we studied such final stages of damage production in GaAs using electron microscopy and X-ray and chemical microanalysis [26]. The AFM

measurements of the array of laser-irradiated GaAs areas showed that the features of nanometer-sized damaged surface regions depended on both the energy density of incident radiation (for $W > W_0$) and the number N of pulsed quasi-static photostrains in the semiconductor. Similar results could be obtained not only by varying N at $W = \text{const}$ but also by increasing W under conditions of $N = \text{const}$. Indeed, an increase in W inevitably resulted in a shift of the aforementioned stages of the defect formation in GaAs to smaller values of N .

4. CONCLUSION

The results obtained make it possible to consider the process of catastrophic damage in micrometer-sized GaAs regions exposed to multiple laser pulses from a unified standpoint; i.e., this process is considered as multistage. The earliest (initial) stages of defect formation in a semiconductor subjected to inelastic deformation ($W > W_0$ [22]) feature the latent buildup of mainly point defects (arsenic vacancies, excess of gallium [26]) from pulse to pulse. As N increases, individual defects merge into nanometer-sized clusters and, thus, form chaotic local depressions in the surface profile and are subsequently involved in orientational self-organization of these clusters. We used the PTSS and AFM methods to show that not only the elevated temperatures or electronic excitation but also the shearing strains $dU_z/dr(r)$ and subsurface stresses contribute significantly to the mechanisms of the defect formation and the clusters' migration [23–25]. The results obtained are consistent with both the quasi-1D electronic–deformational–thermal model of the laser-induced defect production in semiconductors [39–41] and the strain-stimulated “dimensional” effects [23–25, 34, 35].

The consecutive stages of defect formation (monitored for the first time by the AFM method in micrometer-sized GaAs regions) at increasing nanometer-scale surface displacements ΔU_z show clearly (as in the case of Ge [42]) that the processes of self-organization of the defect clusters are gradually transformed into subsequent nanoscale and microscale damage in the semiconductor. We believe that similar mechanisms of defect generation in GaAs can also be encountered in the case of other methods for heating the micrometer-sized semiconductor regions, for example, by passing the electric current through the sample. Thus, the processes studied may give rise to fundamental limitations on the standard operation modes of commercial small-sized devices (Gunn and Schottky diodes and other devices) with local heat release [30] and, correspondingly, with local strains [32] in the active semiconductor layers.

ACKNOWLEDGMENTS

We thank I.E. Sapozhnikov and A.G. Barskov for their help with preparation of some of the samples and with maintenance of the probing lasers.

REFERENCES

1. M. Shur, *GaAs Devices and Circuits* (Plenum, New York, 1987; Mir, Moscow, 1991).
2. A. V. Dvurechenskii, G. A. Kachurin, E. V. Nidaev, and L. S. Smirnov, *Pulse Annealing of Semiconductor Materials* (Nauka, Moscow, 1982).
3. *Semiconductors and Semimetals*, Vol. 23: *Pulsed Laser Processing of Semiconductors*, Ed. by R. F. Wood, C. W. White, and R. T. Young (Academic, New York, 1984).
4. N. G. Dzhumamukhambetov and A. G. Dmitriev, *Pis'ma Zh. Tekh. Fiz.* **17** (13), 21 (1991) [*Sov. Tech. Phys. Lett.* **17**, 467 (1991)].
5. V. D. Andreeva, M. I. Anisimov, N. G. Dzhumamukhambetov, and A. G. Dmitriev, *Fiz. Tekh. Poluprovodn. (Leningrad)* **24**, 1010 (1990) [*Sov. Phys. Semicond.* **24**, 635 (1990)].
6. B. G. Gribov, G. M. Gusakov, T. N. Kondratova, *et al.*, *Dokl. Akad. Nauk SSSR* **314**, 618 (1990) [*Sov. Phys. Dokl.* **35**, 847 (1990)].
7. A. I. Efimova, P. K. Kashkarov, V. I. Petrov, and V. Yu. Timoshenko, *Poverkhnost*, No. 8, 94 (1990).
8. N. G. Dzhumamukhambetov and A. G. Dmitriev, *Fiz. Tekh. Poluprovodn. (Leningrad)* **22**, 1880 (1988) [*Sov. Phys. Semicond.* **22**, 1192 (1988)].
9. G. M. Gusakov, T. N. Kondratova, K. S. Kapskii, and A. I. Laryushin, *Fiz. Tekh. Poluprovodn. (Leningrad)* **23**, 1864 (1989) [*Sov. Phys. Semicond.* **23**, 1154 (1989)].
10. P. K. Kashkarov, V. I. Petrov, D. V. Ptitsyn, and V. Yu. Timoshenko, *Fiz. Tekh. Poluprovodn. (Leningrad)* **23**, 2080 (1989) [*Sov. Phys. Semicond.* **23**, 1287 (1989)].
11. G. D. Ivlev, F. M. Koshchanov, V. L. Malevich, and E. A. Tyavlovskaya, *Pis'ma Zh. Tekh. Fiz.* **16** (6), 42 (1990) [*Sov. Tech. Phys. Lett.* **16**, 222 (1990)].
12. C. Cohen, J. Siejka, and D. Pribat, *J. Phys. Colloq. C5 (Paris)* **44** (10), 179 (1983).
13. K. K. Dzhamanbalin, A. G. Dmitriev, É. N. Sokol-Nomokonov, and Yu. I. Ukhanov, *Fiz. Khim. Obrab. Mater.*, No. 2, 20 (1990).
14. A. G. Dmitriev, *Fiz. Tekh. Poluprovodn. (St. Petersburg)* **27**, 582 (1993) [*Semiconductors* **27**, 323 (1993)].
15. F. A. McDonald, R. J. Gutfield, and R. W. Dreyfus, *Proc.-IEEE Ultrason. Symp.*, 403 (1986).
16. S. V. Vintsents and S. G. Dmitriev, *Zh. Tekh. Fiz.* **67**, 105 (1997) [*Tech. Phys.* **42**, 216 (1997)].
17. S. V. Vintsents, S. G. Dmitriev, and O. G. Shagimuratov, *Fiz. Tverd. Tela (St. Petersburg)* **38**, 993 (1996) [*Phys. Solid State* **38**, 552 (1996)].
18. S. V. Vintsents, S. G. Dmitriev, and K. I. Spiridonov, *Fiz. Tverd. Tela (St. Petersburg)* **39**, 2224 (1997) [*Phys. Solid State* **39**, 1985 (1997)].
19. S. V. Vintsents, S. G. Dmitriev, R. A. Zakharov, and G. S. Plotnikov, *Fiz. Tekh. Poluprovodn. (St. Petersburg)* **31**, 513 (1997) [*Semiconductors* **31**, 433 (1997)].
20. S. V. Vintsents, V. B. Zaitsev, A. V. Zoteyev, *et al.*, in *Proceedings of 3rd International Conference on Physics of Low-Dimensional Structures* (Chernogolovka, 2001), Vol. 3, p. 69.

21. S. V. Vintsents, V. B. Zaitsev, A. V. Zoteev, *et al.*, Fiz. Tekh. Poluprovodn. (St. Petersburg) **36**, 947 (2002) [Semiconductors **36**, 883 (2002)].
22. S. V. Vintsents, A. V. Zoteev, and G. S. Plotnikov, Fiz. Tekh. Poluprovodn. (St. Petersburg) **36**, 902 (2002) [Semiconductors **36**, 841 (2002)].
23. A. G. Barskov and S. V. Vintsents, Fiz. Tverd. Tela (St. Petersburg) **36**, 2590 (1994) [Phys. Solid State **36**, 1411 (1994)].
24. S. V. Vintsents and S. G. Dmitriev, Pis'ma Zh. Tekh. Fiz. **21** (19), 1 (1995) [Tech. Phys. Lett. **21**, 767 (1995)].
25. S. V. Vintsents, S. G. Dmitriev, and O. G. Shagimuratov, Pis'ma Zh. Tekh. Fiz. **22** (8), 8 (1996) [Tech. Phys. Lett. **22**, 602 (1996)].
26. A. G. Barskov, S. V. Vintsents, G. G. Dvoryankina, *et al.*, Poverkhnost, No. 3, 79 (1995).
27. D. V. Lioubtchenko, I. A. Markov, and T. A. Briantseva, Appl. Surf. Sci. **195**, 42 (2002).
28. A. Blazhis, S. Zhilenis, and G. Tautvaishas, Zh. Tekh. Fiz. **58**, 2237 (1988) [Sov. Phys. Tech. Phys. **33**, 1359 (1988)].
29. W. W. Duley, *Laser Processing and Analysis of Materials* (Plenum, New York, 1983).
30. V. I. Borisov, V. E. Lyubchenko, and A. S. Rogashkov, Élektron. Tekh., Ser. 1: Élektron. SVCh **10**, 404 (1987).
31. V. E. Lyubchenko, Radiotekhnika (Moscow), No. 2, 16 (2002).
32. A. L. Polyakova, *Deformation of Semiconductors and Semiconductor Devices* (Énergiya, Moscow, 1979).
33. P. K. Kashkarov, M. V. Rusina, and V. Yu. Timoshenko, Fiz. Tekh. Poluprovodn. (St. Petersburg) **26**, 1835 (1992) [Sov. Phys. Semicond. **26**, 1030 (1992)].
34. C. S. Lee, N. Koumvakalis, and M. Bass, Appl. Phys. Lett. **41**, 625 (1982); Opt. Eng. **22**, 419 (1983); J. Appl. Phys. **54**, 5727 (1983).
35. S. S. Cohen, J. B. Bernstein, and P. W. Wyatt, J. Appl. Phys. **71**, 630 (1992).
36. A. S. Filonov and I. V. Yaminskii, *User's Manual for FemtoSkan-001* (TsPT, Moscow, 1999).
37. Yu. I. Golovin and A. I. Tyurin, Fiz. Tverd. Tela (St. Petersburg) **42**, 1818 (2000) [Phys. Solid State **42**, 1865 (2000)].
38. V. P. Alekhin, *Physics of Strength and Plasticity of Surface Layers of Materials* (Nauka, Moscow, 1983).
39. V. I. Emel'yanov and P. K. Kashkarov, Poverkhnost, No. 2, 77 (1990).
40. V. I. Emel'yanov and P. K. Kashkarov, Appl. Phys. A **55**, 161 (1992).
41. P. K. Kashkarov and V. Yu. Timoshenko, Poverkhnost, No. 6, 5 (1995).
42. S. V. Vintsents, A. V. Zaitseva, and G. S. Plotnikov, Fiz. Tekh. Poluprovodn. (St. Petersburg) **37**, 134 (2003) [Semiconductors **37**, 124 (2003)].

Translated by A. Spitsyn